

Inertial migration of neutrally buoyant particles in a square duct: An investigation of multiple equilibrium positions

B. Chun and A. J. C. Ladd^{a)}

Department of Chemical Engineering, University of Florida, Gainesville, Florida 32611-6005

(Received 18 November 2005; accepted 24 January 2006; published online 16 March 2006)

Inertial migration of neutrally buoyant particles in a square duct has been investigated by numerical simulation in the range of Reynolds numbers from 100 to 1000. Particles migrate to one of a small number of equilibrium positions in the cross-sectional plane, located near a corner or at the center of an edge. In dilute suspensions, trains of particles are formed along the axis of the flow, near the planar equilibrium positions of single particles. At high Reynolds numbers ($Re \geq 750$), we observe particles in an inner region near the center of the duct. We present numerical evidence that closely spaced pairs of particles can migrate to the center at high Reynolds number. © 2006 American Institute of Physics. [DOI: 10.1063/1.2176587]

In Poiseuille flow, a neutrally buoyant particle migrates to a position that is determined by the balance of forces generated by the gradient of the shear rate and interactions of the flow field with the container walls. In a cylindrical flow, uniformly distributed particles migrate to form a stable ring located at approximately $0.6R$, where R is the radius of the cylinder.¹ Theoretical calculations for small particles in planar Poiseuille flow give equilibrium positions similar to those observed experimentally.^{2,3} Asmolov³ extended the method of matched asymptotic expansions² to a higher Reynolds number, obtaining good agreement with experiment⁴ up to $Re = UD/\nu = 1700$, where turbulent flow was first observed. Here, U is the average flow velocity, D is the cylinder diameter, and ν is the kinematic viscosity of the fluid. The profile of the lateral force across the channel shows only one equilibrium position, which shifts closer to the boundary wall as the Reynolds number increases. Our interest in this problem was sparked by two recent experimental observations: first that particles tend to align near the walls to make linear chains of more or less equally spaced particles,^{1,5} and second that at high Reynolds numbers ($Re \sim 1000$), an additional inner ring of particles was observed when the ratio of particle diameter d to cylinder diameter was of the order of $1:10$.⁴ Large particles introduce an additional Reynolds number, $Re_p = Re(d/D)^2$, which may not be small, as assumed theoretically.^{2,3}

In this work, inertial migration of neutrally buoyant particles has been investigated by numerical simulation in the range of Reynolds numbers from 100 to 1000. We have focused on large particles, with a diameter of about $1/10$ of the channel dimension (H). Initially we studied a pressure-driven channel flow, but we found only a single equilibrium position, in close agreement with theory. To investigate the effects of geometry we next studied a square duct, which was simpler for our code than a cylinder. Here we found that an isolated sphere migrates to one of a discrete set of equilibrium positions, depending on initial conditions. We discuss

the evolution of these equilibrium positions with the Reynolds number. In dilute suspensions, we observed linear chains of particles being formed in the flow direction, similar to what has been seen in laboratory experiments.⁵ At higher Reynolds numbers these chains become unstable and break up into small clusters that tend to migrate towards the center of the duct at $Re \sim 1000$. We have attempted to explain this migration by examining the equilibrium positions of dumbbells at different Reynolds numbers.

We have used numerical simulations of single- and multiparticle suspensions to generate the results reported in this paper. The simulations utilized the lattice-Boltzmann method,⁶ with modifications for particle suspensions.^{7,8} Technical details of the method have been given previously;^{8,9} here we focus on three specific issues relevant to the present work. The accuracy of the numerical simulation is controlled by the size of the particle relative to the grid spacing Δx of the underlying lattice. The code was therefore tested with different particle diameters, $d = 5.6\Delta x$, $9.6\Delta x$, and $16.6\Delta x$, in a planar Poiseuille flow where the equilibrium positions are known;³ in each case we kept the ratio d/H the same. We found that when the migration force is weak, the smallest particle did not always reach the correct lateral position. Instead it would become locked onto a specific position related to the fluid grid. This numerical artifact is expected to diminish as the particle gets larger, and indeed the trajectories of particles with $d = 9.6\Delta x$ and $d = 16.6\Delta x$ showed the same final position in all cases, which was in agreement with theory.³ In the duct-flow simulations, we used particles of $9.6\Delta x$, with a limited number of additional simulations using larger particles ($16.6\Delta x$) as a check. The cross section of the duct was set to approximately $9d \times 9d$, and the periodic repeat length in the flow direction (L) was varied between $5d$ and $20d$. In general, our results were insensitive to the length of the periodic cell, and we typically used $L = 5d$ for single-particle simulations, and $L = 20d$ for multiparticle simulations.

We found an additional equilibrium position at the center of the channel if the Mach number of the flow was larger

^{a)}Electronic address: ladd@che.ufl.edu

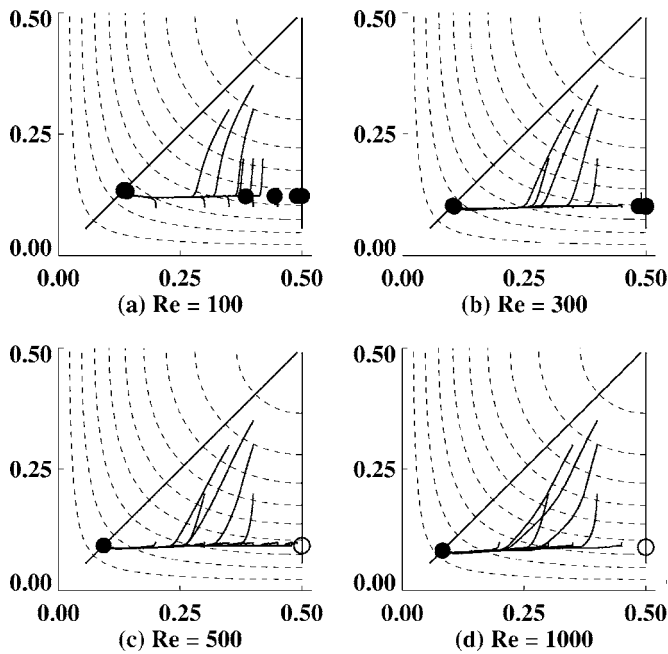


FIG. 1. The trajectories of individual particles projected onto the velocity gradient plane, perpendicular to the direction of flow. Distance is normalized by the width of the duct, and all the figures are one-quarter of the total cross section. The dashed lines are isocontours of the flow velocity, and particle trajectories are shown as solid lines. The solid circles are the final positions of each trajectory, and open circles are unstable equilibrium positions.

than 0.1, regardless of the particle size. As yet, we do not know if this is a physical effect of the finite compressibility fluid or a numerical artifact. However, to avoid this issue, we kept the Mach number (Ma) less than 0.05 in all cases, which is rather smaller than the usual incompressible flow limit ($Ma < 0.3$). Finally, we observed a small secondary flow, which is clearly a numerical artifact. Laminar flow in a square duct is stable at all Reynolds numbers,¹⁰ but, because of the finite grid size, perturbations to the flow occur at the corners and then propagate into the bulk. The secondary flow velocity scales as $U \text{Re}(\Delta x/H)^2$, and thus the ratio of the inertial migration velocity,³ $u \sim \text{Re}(d/H)^3$, to the secondary flow velocity is $\alpha d^3/(\Delta x^2 H)$. The coefficient α lies between 10^2 and 10^4 depending on the particle position in the duct. We chose a duct large enough so that the secondary flow can always be neglected. Typical values in our simulations, $H = 100\Delta x$ and $d = 9.6\Delta x$, give an artificial migration due to the secondary flow less than 1% of the inertial migration.

The trajectories of a single particle, illustrated in Fig. 1, show that the force has components perpendicular to the contour lines of the flow field and the boundary of the duct. Particles migrate to one of a small number of equilibrium positions in the cross-sectional plane, located near a corner or at the center of an edge. In all cases the stable particle positions are close to the wall, approximately $0.2H$ away, where H is the width of the duct, similar to the position found experimentally.¹ We have observed up to eight symmetrically placed equilibrium positions for the particles, which reflect the broken symmetry of the duct compared with a cylinder. A particle beginning along one of the symmetry lines goes directly to its equilibrium position, while a

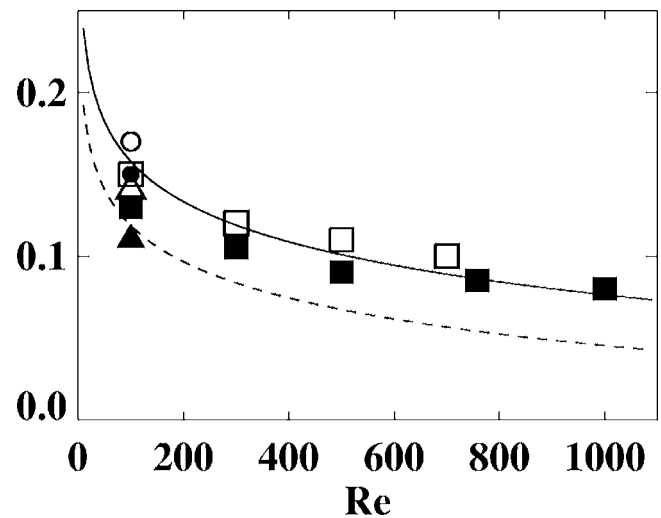


FIG. 2. Equilibrium distance of a single particle from the wall in units of the width of the duct. The open symbols are for planar Poiseuille flow, while the solid symbols indicate different H to d ratios: triangles— $H/d=16.1$, squares— $H/d=9.1$, and circles— $H/d=5.6$. The solid line is a fit to experimental results for Poiseuille flow with $D/d=9$ (Ref. 4). The dashed line is the prediction of the asymptotic theory for planar Poiseuille flow with $H/d \rightarrow \infty$ (Ref. 3).

particle beginning in an asymmetric location migrates in two stages. In the first stage it moves along a line that crosses contours of the fluid velocity at right angles, and in the second stage it moves along a line parallel to a boundary wall towards the nearest corner. The time to steady state is of the order of $10\,000t_s$, where $t_s = d/2U$ is the Stokes time. The migration velocity depends on the distance from the corner and the angle between its trajectory and the wall. The first stage is a relatively fast process, taking less than $3000t_s$ even at the lowest Reynolds number, $\text{Re}=100$. The second stage of migration is slower, taking up to $10\,000t_s$ at $\text{Re}=100$. At higher Reynolds numbers the migration is faster; at $\text{Re}=500$, the times are $2500t_s$ and $4000t_s$, respectively. Laboratory experiments have used cylinders of lengths $200d-4000d$,¹ and $2000d-20\,000d$,⁴ which suggests that in some cases the particles may not have reached their steady-state positions.

To illustrate the migration paths we chose several representative initial positions, located in a quadrant of the velocity gradient plane. Trajectories at different Reynolds numbers in the range $100 \leq \text{Re} \leq 1000$ are shown in Fig. 1. At $\text{Re}=100$ [Fig. 1(a)], the corners $(0.13, 0.13)$ and a region near the middle of one face $(0.38-0.5, 0.13)$ are stable equilibrium positions. However, the length of the stable central region decreases with increasing Reynolds number [Fig. 1(b)] and vanishes at $\text{Re}=500$ [Fig. 1(c)]. At Reynolds numbers of 500 [Fig. 1(c)], and 1000 [Fig. 1(d)], only the corner positions are stable. There is always an equilibrium point at the exact center of the face, but it is an unstable equilibrium above $\text{Re}=500$.

Figure 2 shows the distance between a particle and the nearest boundary. The particles move closer to the wall with increasing Reynolds number, in agreement with theory³ and experiment.⁴ Results for a square duct with $H/d=9.1$ are similar to experimental results in a cylindrical Poiseuille

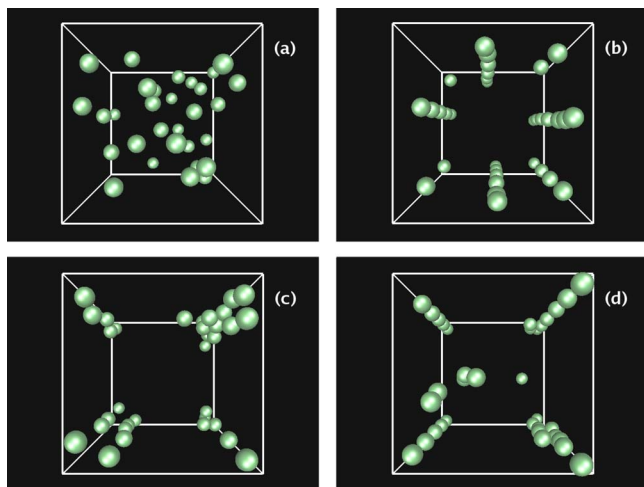


FIG. 3. Snapshots of particle configurations in a duct flow at different Reynolds numbers; the flow is into the plane of the paper. The ratio $H/d=9.1$, the number of particles $N=32$, and the volume fraction $\phi=1\%$.

flow with $D/d=9$. The small deviation between the simulation and experiment can be explained by the curvature of cylinder. The equilibrium position in a channel flow is slightly farther from the wall than in a duct flow, but the large systematic deviation between theory and simulation is due to the finite particle size and the non-negligible inertia on the particle scale ($1 \leq \text{Re}_p \leq 10$). In general, the equilibrium position is shifted farther from the wall with increasing particle size, but gets closer to the wall with increasing Re .

In order to simulate multiparticle suspensions, random configurations were prepared with a volume fraction $\phi=1\%$ and size ratio $H/d=9.1$. The Reynolds number in the simulations varied between 100 and 1000. An initially uniform distribution, shown in Fig. 3(a), evolves into three different steady-state distributions depending on Re . At $\text{Re}=100$ [Fig. 3(b)], particles are gathered around the eight equilibrium positions and are strongly aligned in the direction of the flow, making linear chains of more or less uniformly spaced particles. Similar trains of particles were observed in recent laboratory experiments.⁵ At $\text{Re}=500$ [Fig. 3(c)], the particles are gathered in one of the four stable positions near each corner. When the Reynolds number reaches 500, the trains are unstable and the spacing between the particles is no longer uniform. Instead, transient aggregates of closely spaced particles are formed, again near the corners of the duct. However, at still higher Reynolds number ($\text{Re}=1000$), there is another change in particle configuration [Fig. 3(d)], where particles appear in the center of the duct. A central band was first observed in experiments in a cylindrical flow,⁴ but its origin remains unclear. We observe that the central particles have a substantial diffusive motion in the velocity-gradient plane, whereas the particle trains exhibit little transverse diffusion. Since there are no single-particle equilibrium positions at the duct center, the presence of particles in the inner region is clearly due to multibody interactions. Nevertheless, this migration cannot be a shear-induced migration of the kind that occurs in low-Reynolds-number flows.¹¹

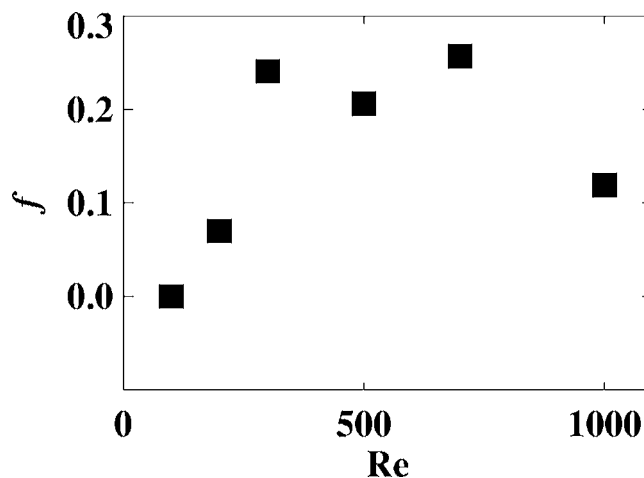


FIG. 4. The time-averaged fraction of particles forming hydrodynamic clusters (f); a cluster is defined by a group of particles with separations less than $1.1d$.

A scaling analysis implies that the relative magnitude of hydrodynamic diffusion compared to inertial migration decays upon increasing the Reynolds number. When the volume fraction of suspended particles is fixed, the diffusivity due to shear-induced migration is proportional to $\dot{\gamma}d^2$,¹² so that the corresponding velocity of migration from high to low shear is $\sim U(d/H)^2$, where the local shear rate $\dot{\gamma}$ can be taken to be of order U/H . Therefore, the relative magnitude of inertial and shear induced migration is $\sim \text{Re}(d/H)$. Thus, shear-induced migration would be expected to become negligible in comparison with inertial migration at sufficiently high Re . However, we observe enhancement of dispersion at higher Re , which indicates a different dispersive mechanism.

Even though the suspensions are dilute and there are no attractive forces, clusters of particles are observed at Reynolds numbers greater than 300. Below $\text{Re}=300$, stable linear chains of particles are formed at the planar equilibrium positions, with particles more or less uniformly spaced in the flow direction. As the Reynolds number increases, the spacing in the flow direction becomes irregular and clusters are formed. We define a cluster as a group of particles with surfaces separated by a gap of no more than $0.1d$. Figure 4 shows a sharp increase in the clustered fraction at Reynolds numbers between $\text{Re}=200$ and $\text{Re}=300$, consistent with the snapshots in Fig. 3. At $\text{Re}=1000$, about 12% of the particles form clusters, corresponding to 3–4 particles out of the 32 particles in the system.

Despite the prevalence of hydrodynamic clusters at Reynolds numbers as low as 300, it is not until $\text{Re} \sim 1000$ that particles appear in the center of the duct. In an attempt to understand the high- Re migration towards the center, we have investigated the migration and equilibrium position of isolated pairs of particles. A dumbbell was constructed by connecting two particles with a stiff spring; the force-free separation of the pair was $1.05d$. Figure 5 shows that at $\text{Re}=100$, the equilibrium position of a dumbbell is similar to that of a single particle: less than $0.2H$ from the wall. The dumbbell is located slightly farther from the wall since it is effectively a larger particle. The dumbbell moves slightly

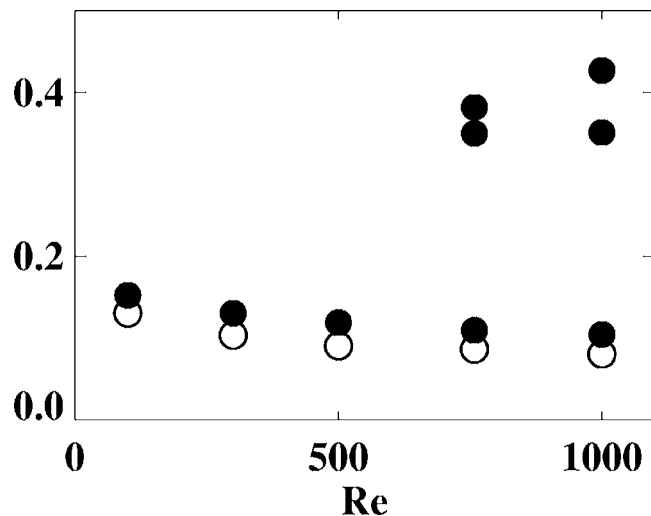


FIG. 5. Equilibrium center-of-mass position of a single particle and a dumbbell, scaled by the duct width, H . The open circles are the equilibrium positions of a single particle and the solid circles are the equilibrium position of a dumbbell with a separation of $1.05d$ between the spheres.

closer to the wall as the Reynolds number increases, just like a single particle. However, at $Re > 700$, there is a sudden onset of additional equilibrium positions near the center of the duct. Thus, clustered particles stay near the corner at $Re \leq 500$, but move to the inner region at $Re = 1000$. At volume fractions less than 0.5%, we do not observe any inner band of particles nor any cluster formation, which further indicates a connection between the migration of clusters and the presence of particles in the inner region.

Our results therefore suggest the following sequence of events in dilute suspensions of large particles. At low Reynolds numbers, the particles migrate to a position near the boundary walls. The particles are evenly spaced in the flow direction, forming the linear chains observed both numerically and experimentally. At higher Reynolds numbers, the uniform spacing is broken and closely spaced pairs and triplets are formed. These clusters have additional equilibrium positions near the center of the duct at sufficiently high Reynolds number ($Re > 700$). Once in the center they form a diffuse layer, in contrast to the much more tightly locked bands near the boundary.

In conclusion, we have examined the inertial migration

of neutrally buoyant particles in a square duct, at Reynolds numbers between 100 and 1000. The trajectories of single particles show migration directed perpendicular to the constant velocity flow lines and to the boundary walls. The equilibrium positions are determined by the interplay between the background flow field and the square shape of the boundary. In dilute suspensions we observed symmetrically placed equilibrium positions rather than a ring of particles as in a cylindrical Poiseuille flow. We also observed a cloud of particles in an inner region at $Re = 1000$ and volume fractions in excess of 1%. This inner group of particles results from the formation of hydrodynamic clusters, which then migrate to the center. We have shown that the closely spaced pairs of particles have new equilibrium positions near the center of the duct at $Re > 700$. We believe these observations will prove relevant in interpreting the results of recent experiments.⁴

This work was supported by the National Aeronautics and Space Administration, Grant No. NAG NNCO4GA89G.

¹G. Segre and A. Silberberg, "Behaviour of macroscopic rigid spheres in Poiseuille flow: Part 2. Experimental results and interpretation," *J. Fluid Mech.* **14**, 136 (1962).

²J. A. Schonberg and E. J. Hinch, "Inertial migration of a sphere in Poiseuille flow," *J. Fluid Mech.* **203**, 517 (1989).

³E. S. Asmolov, "The inertial lift on a spherical particle in a plane Poiseuille flow at large channel Reynolds number," *J. Fluid Mech.* **381**, 63 (1999).

⁴J. Matas, J. F. Morris, and E. Guazzelli, "Inertial migration of rigid sphere particles in Poiseuille flow," *J. Fluid Mech.* **515**, 171 (2004).

⁵J. Matas, V. Glezer, E. Guazzelli, and J. Morris, "Trains of particles in finite-Reynolds-number pipe flow," *Phys. Fluids* **16**, 4192 (2004).

⁶F. J. Higuera and J. Jimenez, "Boltzmann approach to lattice gas simulations," *Europhys. Lett.* **9**, 663 (1989).

⁷A. J. C. Ladd, "Numerical simulations of particulate suspensions via a discretized Boltzmann equation. Part I. Theoretical foundation," *J. Fluid Mech.* **271**, 285 (1994).

⁸A. J. C. Ladd and R. Verberg, "Lattice-Boltzmann simulations of particle-fluid suspensions," *J. Stat. Phys.* **104**, 1191 (2001).

⁹N. Q. Nguyen and A. J. C. Ladd, "Lubrication corrections for lattice-Boltzmann simulations of particle suspensions," *Phys. Rev. E* **66**, 046708 (2002).

¹⁰T. Tatsumi and T. Yoshimura, "Stability of the laminar flow in a rectangular duct," *J. Fluid Mech.* **212**, 437 (1990).

¹¹M. Frank, D. Anderson, E. R. Weeks, and J. F. Morris, "Particle migration in pressure-driven flow of a Brownian suspension," *J. Fluid Mech.* **493**, 363 (2003).

¹²D. Leighton and A. Acrivos, "The shear-induced migration of particles in concentrated suspensions," *J. Fluid Mech.* **181**, 415 (1987).